Published in final edited form as:
J Immunol. 2013 August 15; 191(4): . doi:10.4049/jimmunol.1300479.

IL-17RA is Essential for Optimal Localization of Follicular T Helper Cells in the Germinal Center Light Zone to Promote Autoantibody-Producing B cells[1]

Yanna Ding[*,†], **Jun Li**[*], **Qi Wu**[*], **Pingar Yang**[*], **Bao Luo**[*], **Shutao Xie**[*], **Kirk M. Druey**[§], **Allan J. Zajac**[‡], **Hui-Chen Hsu**[*,‖], and **John D Mountz**[*,¶,‖]

[*]Department of Medicine, University of Alabama at Birmingham, Birmingham, AL

[†]Department of Pathology, University of Alabama at Birmingham, Birmingham, AL

[‡]Department of Microbiology, University of Alabama at Birmingham, Birmingham, AL

[§]National Institute of Allergy and Infectious Diseases, Bethesda, MD

[¶]Birmingham VA Medical Center, Birmingham, AL, 35294

Abstract

Germinal centers provide a microenvironment that promotes and regulates the interactions of B-cells with follicular T-helper cells (T_{FH}). Here we show that there are significantly higher frequencies of $CXCR5^+ICOS^+T_{FH}$ cells in autoimmune BXD2 mice, and these cells express both interleukin (IL)-21R and IL-17RA. Although IL-17 and IL-21 are both important for the formation of spontaneous GCs and development of pathogenic autoantibodies, IL-21, but not IL-17, is required for the proper development of T_{FH} cells in BXD2 mice. The total numbers of T_{FH} cells and their ability to induce B cell responses *in vitro* were not affected by a deficiency of IL-17RA in BXD2-*Il17ra*$^{-/-}$ mice, the majority of $CXCR5^+$ T_{FH} cells from BXD2-*Il17ra*$^{-/-}$ mice were, however, not localized in the GC light zone (LZ). Interruption of IL-17 signaling, either acutely by AdIL-17R:Fc or chronically by *Il17ra*$^{-/-}$, disrupted T_{FH}–B interactions and abrogated the generation of autoantibody-forming B cells in BXD2 mice. IL-17 upregulated the expression of regulator of G-protein signaling (RGS)16 to promote the ability of T_{FH} to form conjugates with B cells which was abolished in T_{FH} cells from BXD2-*Rgs16*$^{-/-}$ mice. The results suggests that IL-17 is an extrinsic stop signal that it acts on post-differentiated $IL\text{-}17RA^+$ T_{FH} to enable its interaction with responder B cells in the LZ niche. These data suggest a novel concept that T_{FH} differentiation and its stabilization in the LZ are two separate checkpoints and that IL-21 and IL-17 act at each checkpoint to enable pathogenic GC development.

Introduction

Germinal centers (GCs) are essential in promoting T-dependent immune responses (1, 2). They provide a microenvironment that promotes and regulates the interactions of B-cells with follicular T-helper cells (T_{FH}), which provide the cognate help required for the generation of high-affinity, antibody-producing plasma cells and memory B cells (3, 4).

[1]This work is supported by grants from VA Merit Review Grant (1I01BX000600-01), NIH/NIAID (1AI 071110, ARRA 3RO1AI71110-02S1,1RO1 AI083705, and U01 AI082966), American College of Rheumatology (ACR)-Within-Our-Reach, Rheumatology Education Foundation, Alliance for Lupus Research, Arthritis Foundation, Lupus Research Institute, and, in part, by the Intramural Research Program of the NIAID, NIH.

[‖]Corresponding author: Hui-Chen Hsu, PhD, SHEL 311, 1825 University Blvd, Birmingham, AL 35294; Phone: 205-934-8909, Fax: 205-996-6788, rheu078@uab.edu; John D. Mountz, MD, PhD, SHEL 307, 1825 University Blvd, Birmingham, AL 35294; Phone: 205-934-8909, Fax: 205-996-6788, jdmountz@uab.edu.

Spontaneous GC formation has been demonstrated in various mouse models of autoimmune disease (5), and dysregulated GC formation or function may contribute to autoimmune disease in humans (6, 7). Dysregulation of GCs is often caused by aberrant accumulation or function of T_{FH} cells (8, 9), and an increase in the numbers of T_{FH} cells has been correlated with the severity of disease in several autoimmune conditions, including systemic lupus erythematosus (SLE) (10-12). In mouse models of lupus, the elimination or defective function of GC T_{FH} cells reduces or even abolishes the disease (5, 13).

High levels of IL-21 are found in the circulation of patients with SLE (14), and disruption of IL-21 signaling can inhibit GC formation and autoantibody production as well as ameliorate autoimmune disease in mice (15). Although IL-21is important but not necessarily essential for T_{FH} development (16-18), IL-21 is considered a signature cytokine of T_{FH} cells (15, 19, 20). IL-21 acts in an autocrine manner to stimulate the proliferation and survival of T_{FH} cells, and hence has a direct effect on their accumulation and the associated formation of GCs (21, 22). IL-21 directly induces high expression of Bcl6, the master transcription factor for T_{FH} differentiation, which is important for the sustained expression of CXCR5 and also promotes the expression of other T_{FH} co-stimulatory molecules supporting cognate help to B cells (20, 23, 24). The CXCL13–CXCR5 interaction mediates the migration of T_{FH} cells to the GC light zone (LZ)where the affinity maturation of B cells takes place (25, 26).

Until recently, the potential role of IL-17A in GC formation and function received less attention, as T_{FH} cells has been shown to not to produce IL-17A (19). High levels of IL-17 and T_H17 cells are commonly found in patients with autoimmune disease (27) and have now been shown to drive GC and ectopic lymphoid follicle development in mouse models of autoimmune disease (28, 29). Using the BXD2 model of systemic autoimmune disease, we established that T_H17 cells can be identified in the spontaneous GCs (28, 30) and that IL-17 promotes the formation of GCsin these mice (28). Analysis of the effects of IL-17 on B cells in the GCs indicate that it modulates the expression of regulator of G protein signaling (RGS) proteins, which promote desensitization of B cell chemotaxis to chemokines CXCL12 and CXCL13 and stabilization of interactions of the GC B cells with nearby T-helper cells (31).

IL-17A signals through the IL-17RA–IL-17RC heterodimeric receptor complex (32). The original cloning of IL-17RA revealed that T cells as well as B cells can express high levels of *Il17ra* and can be responsive to IL-17 stimulation (33). Although it has been demonstrated that IL-17 is not required for the development of T_{FH} cells (22) but may be involved in antibody production (29, 34), the possibility that IL-17 can act cooperatively with IL-21 to affect the function of T_{FH} cells in regulating GC responses has not been explored. Here, we provide evidence that, compared with normal B6 mice, there are significantly higher frequencies of T_{FH} cells in autoimmune BXD2 mice, and these cells express high levels of both IL-21R and IL-17RA. Although T_{FH} was dramatically deficient in BXD2-*Il21*$^{-/-}$ mice, the percentage and the direct B-cell support function of T_{FH} were not affected by IL-17RA deficiency. We have established that the IL-17RA signal is important for securing the localization of T_{FH} in the GC LZ in BXD2-*Il17ra*$^{-/-}$ mice. Such anatomic stabilization is needed for T_{FH} to induce its function and hence is a unique T_{FH} checkpoint in autoreactive GCs.

Materials and Methods

Mice

C57BL/6 (B6) and BXD2 recombinant inbred mice were obtained from The Jackson Laboratory, B6-*Il17ra*$^{-/-}$ mice were obtained from Amgen, Inc. (Thousand Oaks, CA), B6-*Rgs16*$^{-/-}$ mice were a gift from Dr. Kirk M. Druey, and B6-*Il21*$^{-/-}$ mice were obtained from

the Mutant Mice Regional Resource Center (Davis, CA). These mice were backcrossed with BXD2 mice for seven generations by a marker-assisted speed congenic approach. All mice were housed in the University of Alabama at Birmingham (UAB) Mouse Facility under specific pathogen-free conditions in a room equipped with an air-filtering system. The cages, bedding, water, and food were sterilized. All mouse procedures were approved by The UAB Institutional Animal Care and Use Committee.

Administration of AdLacZ and AdIL-17R:Fc

AdIL-17R:Fc and AdLacZ (2×10^9 p.f.u. per mouse), generous gifts from Dr. Jay Kolls (University of Pittsburgh) (35), were administered intravenously (i.v.). Spleen tissue and cells were analyzed 10 days later.

T cell adoptive transfer

Effector T cells ($CD62L^{-/lo}$ CD4 T) from BXD2 and BXD2-*Rgs16*$^{-/-}$ mice were sorted by FACSAria II and i.v. injected into BXD2-*Il17ra*$^{-/-}$ mice (3×10^6 cells in 200 μl PBS per mouse). Recipients were sacrificed on Days 6 and 21. Spleen tissue and spleen cells were collected for the indicated analysis.

NP-CGG immunization

B6 and B6-*Il17ra*$^{-/-}$ mice were immunized i.p. with 50 μg of NP–chicken gamma globulin (NP-CGG; BioSearch Technologies, Novato, CA) adsorbed to 1.3 mg alum (Sigma-Aldrich) in a total volume of 100 μl NP-CGG alum/PBS. Mice were sacrificed on day 6, 9 and 12. Spleen tissue and spleen cells were collected for the indicated analysis.

Flow cytometry analysis

Single-cell suspensions of whole-spleen cells or migrated cells collected from the lower chamber in a cell migration assay were labeled by surface staining with the following antibodies: Pacific blue– or Alexa488– (RM4-5, GK1.5, Biolegend) or PE–anti-CD4 (RM4-5, Biolegend); Pacific blue–anti-CD19 (6D5, Biolegend); Alexa647–anti-GL-7 (GL7, eBioscience); APC–anti-B220 (RA3-6B2, Biolegend); PE–Cy7-anti-CXCR5 (2G8, BD Biosciences); FITC– or PE– (398.4A, 7E.17G9, eBioscience) or PE–Cy5-anti-ICOS (15F9, Biolegend). Antibodies against PD-1 (RMP1-30, Biolegend), CD28 (37.51, eBioscience), CD40L (MR1, eBioscience), CD62L (MEL-14, BD Biosciences), CD44 (IM7, Biolegend), IL-21R (eBio4A9, eBioscience), IL-17RA (PAAJ-17R, eBioscience), and Fas (15A7, eBioscience) were all conjugated with PE. Peanut agglutinin (PNA) was conjugated with biotin (Vector Laboratory, Burlingame, CA) and was detected by Alexa450-conjugated streptavidin (Invitrogen).

For nuclear transcription factor staining, cells were labeled with surface markers, then fixed and permeabilized with the FoxP3 Staining Buffer Set (eBioscience), according to the manufacturer's instruction. Permeabilized cells were stained with PE–anti-Bcl6 (K112-91, BD Biosciences) and PE–anti-RORγt (Q31-378, BD Biosciences).

For cytokine-producing T cell analysis, cells were stimulated for 5 h with phorbol myristate acetate (PMA; 50 ng/ml; Sigma-Aldrich) and ionomycin (750 ng/ml; Sigma-Aldrich) in the presence of GolgiPlug (BD Biosciences). Cells were stained for surface markers and then fixed and permeabilized with Cytofix/Cytoperm solution (BD Biosciences) before intracellular staining with APC–anti-IL-17 (eBio17B7, eBioscience) and rmIL21R/h-Fc chimera (R&D Systems), followed by R-PE-conjugated goat anti-human IgG (Jackson Immunoresearch) (36). Cell staining profiles were acquired with an LSRII FACS analyzer (BD Biosciences), and data were analyzed with FlowJo software (Tree Star, Inc. Ashland, OR, USA).

Except for T/B conjugates analysis, all flow cytometry analysis was carried out using a combination use of FSC and SSC height, area, and width parameters to exclude aggregated cells.

Immunofluorescent staining of frozen sections

Spleens from mice were collected, embedded in Frozen Tissue Media (Fisher Scientific), and snap-frozen in 2-methylbutane. Frozen sections (8-μm thick) were fixed and processed as previously described (28). Unless specified, all reagents and antibodies were purchased from Invitrogen: Biotin–PNA (Vector Laboratory) followed by SA–Alexa 350; Alexa 555–anti-IgM; Alexa 488–anti-CD35/21 (clone 8C12, BD Bioscience); Dylight 649–goat-anti-mouse IgG (Poly4053, Biolegend); Alexa 647–anti-CD4 (GK1.5, Biolegend); rat anti-mouse-CXCR5 (2G8, BD) followed by goat anti-rat IgG–biotin (Southern Biotech) and SA–Alexa488; rat anti-IL-17 (TC11-18H10.1, Biolegend) and Alexa 555–goat-anti-rat IgG (A21434); goat anti-mouse IL-21 (AF594, R&D Systems) and anti-IL-17R (AF448, R&D Systems) followed by Alexa 647-donkey-anti-goat IgG. Application of chicken anti-mouse RGS16 (NB300-350, Novus Biologicals) and goat anti-chicken IgY–HRP (ab6877, Abcam) was followed by the tyramide signal amplification method (TSA Kit, T20931) and SA–Alexa-488. Sections were mounted in the Slow Fade Gold Antifade reagent and images were captured with a Leica DMIRBE inverted Nomarski/epifluorescence microscope outfitted with Leica TCS NT laser confocal optics. Confocal imaging intensity analysis was carried out using ImageJ software, version 1.4, developed by the U.S. National Institutes of Health (and available on the Internet at http://rsb.info.nih.gov/nih-image/), with background intensity subtracted from each image.

Analysis of T_{FH}–B cell conjugates

Cells were labeled with fluorochrome antibodies against CD3, CD4, B220, CD19, CXCR5, ICOS, and IL-17RAas needed. For T/B conjugates analysis, the doublets based on FSC and SSC height, area and width were included before gating on $CD3^+CD4^+$ cells. The phenotypes of CD4 T cells forming conjugates with B cells were then identified by FACS sorting of$CD4^+B220^+$ or $CD4^+CD19^+$ doublets. The collected conjugates were dissociated with 2 mM EDTA/PBS, as described (37). Cells were then washed and resuspended for flow cytometry acquisition of the cell population distribution.

Real-time quantitative RT-PCR to detect *Rgs16*

RNA isolation, cDNA synthesis, and real-time PCR reactions were carried out as we described previously (28). The following primers were used: *Rgs16*, 5′-GGTACTTGCTACTCGCTTTTCC-3′ (F), 5′-CAGCCGCGTCTTGAACTCT-3′ (R); *Gapdh*, 5′-AGGTCGGTGTGAACGGATTTG-3′ (F), 5′-TGTAGACCATGTAGTTGAGGTCA-3′ (R).

Western blot analysis for RGS16 in CD4 T cells

Spleen $CD4^+$ T cells from BXD2 mice were purified using a MACS column (Miltenyi Biotech) and cultured with either medium alone or with rmIL-17 (30 ng/ml, R&D Systems) for 1 or 24 h. Collected cells were subjected to protein extraction and western immunoblot analysis using the method we described previously (31). Chicken anti-mouse RGS16 (NB300-350, Novus Biologicals) was used at 1:2000 followed by goat anti-IgY–HRP (ab6877, Abcam) at 1:1000. Rabbit anti-mouse GAPDH was used at 1:5000 followed by anti-rabbit HRP-conjugated Ab (Cell Signaling Technology) at a 1:3000 dilution. HRP Abs were detected using chemiluminescence reagent (Pierce).

ELISA

Serum levels of autoantibodies and total IgG levels in cultured supernatant were determined by ELISA, as we described previously (38). BiP was purchased from Assay Designs, Inc. and all other autoantigens from Sigma-Aldrich. Urinary albumin was analyzed using the competitive Albuwell M ELISA kit (Exocell, Inc.), as described previously (38).

ELISPOT quantification of autoantibody-producing B cells

The ELISPOT procedure was carried out using the method we previously described (30). Briefly, polyvinylidene difluoride-backed 96-well plates (Millipore) were coated overnight at 4°C with 5 mg/ml of the indicated autoantigen. BiP was purchased from StressMarq Biosciences Inc. (Victoria BC, Canada), NP_7-BSA was purchased from BioSearch Technologies, and all other autoantigens were purchased from Sigma-Aldrich. Total spleen cells in 100 μl complete medium, containing 5×10^5 cells per well for detecting IgM and 2×10^6 per well for detecting IgG, were cultured overnight in a 37°C incubator. Plated cells were then incubated at RT with HRP-labeled goat anti-mouse IgG/M (Southern Biotechnology) in PBS with 1.5% BSA for 3–4 h. Spots were developed with 3-amino-9-ethylcarbazole. Plates were read by an automatic ELISPOT reader (CTL) and analyzed with Immunospot 3.1 software (CTL).

Cell migration assay

Single-cell suspensions of spleen CD4 T cells were purified using a MACS column (Miltenyi Biotech) and stimulated with medium alone or with mrIL-17 (30 ng/ml, R&D Systems) for 3 h. The cell migration assay was carried out as described (39). The stimulated cells (2×10^6) were loaded into the upper well insert (5-μm pore size) of a Transwell system (Costar), and medium alone or medium with CXCL13 (100 ng/ml, R&D Systems) was added to the bottom chamber. After incubation for 2 h at 37°C in an incubator, the cells that had migrated down to the lower chamber were collected and counted, and the percentage of $CXCR5^+ICOS^+$ CD4 T cells (T_{FH}) was determined by flow cytometry in some experiments. The chemotaxis index of total CD4 T cells or T_{FH} cells was calculated by dividing the number of cells that migrated in the presence of CXCL13 by the number of cells that migrated in the absence of CXCL13 (39).

T_{FH}–B cell coculture, proliferation assay by the Click-iT® EdU assay and IgG secretion detection

Anti-CD19 MACS column (Miltenyi Biotech)-purified B cells from BXD2 were co-cultured in a 3:1 ratio with FACS sorted T_{FH} cells and other CD4 T subsets based on CXCR5 and ICOS expression. T cells were stimulated with anti-CD3 (1 μg/ml) and anti-CD28 (2 μg/ml). T cells and B cells were co-cultured for 2–3 days. One hour before collection, 5-ethynyl-2′-deoxyuridine (EDU, Invitrogen) was added to the cell culture. EDU intensity together with anti-B220 and anti-Thy1.2 staining were determined by flow cytometry analysis, according to the manufacturer's instructions. For analysis of Ig secretion, T cells and B cells were co-cultured for 3 days, supernatant was collected and total IgG were detected by ELISA.

Histology assessment of kidney tissue sections

Kidney tissues collected from the mice were fixed in 10% buffered formalin and then processed to make a paraffin-embedded block. Tissue sections (5 μm) were stained with hematoxylin and eosin (H&E) and examined by light microscopy.

Statistical analysis

All results are shown as the mean ± standard deviation (s.d.). A two-tailed t test was used when two groups were compared for statistical differences. An ANOVA test was used when

more than two groups were compared for statistical differences. P values less than 0.05 were considered significant.

Results

T_{FH} cells express IL-17RA in BXD2 mice

BXD2 mice spontaneously develop a lupus-like syndrome with high titers of autoantibodies and lupus nephritis (30, 40). The disease manifests with age and correlates with the formation of GCs in the spleen (31, 41). At 10 to 12 weeks of age, the mice have well-defined GCs with a prominent LZ and dark zone (DZ) (28, 41). Analysis of the $CD4^+$ T cells in the spleens of BXD2 mice of this age indicated that the frequency and cell count of $CXCR5^+ICOS^+$ $CD4^+$ T cells was significantly higher than in B6 mice (Fig.1A, 1B, Supplementary Fig.1A, 1B). This subpopulation of cells expressed higher levels of PD-1, CD28, CD40L, CD44, IL-21R, (Fig.1C, Supplementary Fig.1C), and Bcl6 (Fig. 1D) but lower levels of CD62L than $CXCR5^-ICOS^-$ and $CXCR5^+ICOS^-CD4^+$ T cells. Approximately 60–70% of the $CXCR5^+ICOS^+$ $CD4^+$ T cells expressed Bcl6, and the highest frequency of cells expressing IL-21 was found in this subpopulation of $CD4^+$ T cells (Fig.1E, Supplementary Fig.1D, 1E). A subpopulation of the $CXCR5^+ICOS^+$ $CD4^+$ T-cell population expressed RORγt (Fig. 1D) and IL-17 (Fig.1E). The $CXCR5^-ICOS^+$ subpopulation of CD4 T cells predominately expressed IL-17 and contained a population of $ROR\gamma t^+$ cells (Fig. 1D, 1E, Supplementary Fig. 1E). However, very few cells in either subpopulation expressed both cytokines (Fig. 1E). The percentage of $IL\text{-}17^+$ or $IL\text{-}21^+$ cells from either subpopulation was significantly higher in BXD2 mouse spleen compared with B6 (Supplementary Fig. 1D, 1E). The current results show that IL-17 and IL-21 are produced from two distinct populations of CD4 T cells and that a subset of T_{FH} cells in the GCs of BXD2 mice may express IL-17 rather than IL-21.

On analysis of the $CXCR5^+$ $CD4^+$ cells in the spleens of BXD2 mice, we found that a very high percentage (~80–90%) of these cells expressed IL-17RA (Fig. 1C, Supplemental Fig. 1C), which indicates that the T_{FH} cells in the spleen of BXD2 mice can potentially respond to IL-17. By confocal microscopic analysis of spleen sections, we found that the LZ contained an apparent population of $CD4^+$ T cells in close proximity to $CD35^+$ follicular dendritic cells (FDCs), with a distinct CD4 T cell zone located adjacent to the dark zone (DZ) of the GC (Fig. 1F). The majority of CD4 T cells localized in the LZ end of the GC were $CXCR5^+$ (arrows indicated, yellow color, Fig.1G). CD4 T cells localized to the LZ of the GC also expressed IL-21 (Fig. 1H), IL-17 (Fig. 1I), and IL-17RA (Fig. 1J). These results demonstrate that there was a distinct population of $CXCR5^+CD4^+$ T cells in the LZ that express IL-17RA and either IL-21 or IL-17 in the BXD2 mice. Such IL-17 producing T cells may represent a unique population of IL-17 producing T_{FH}, as identified by their surface phenotype and location.

Deficiency of either IL-21 or IL-17RA compromises GC development

Although it is shown that blockade of IL-21 or IL-17 signaling can affect GC formation and ameliorate autoimmune disease, it is not known whether the effects of the two cytokines on these aspects of the immune response are identical in BXD2 mice. To answer this question, we generated BXD2-*Il17ra*$^{-/-}$ and BXD2-*Il21*$^{-/-}$ mice. Compared with wild-type BXD2 (BXD2-WT) mice, there were lower levels of anti-histone and anti-DNA autoantibodies of the IgM, IgG2b, and IgG2c isotype in both BXD2-*Il17ra*$^{-/-}$ and BXD2-*Il21*$^{-/-}$ mice (Fig. 2A). Kidney disease, as determined by the levels of urinary albumin (Fig. 2B), the extent of inflammatory infiltrates (Fig. 2C), and IgG deposition in kidney glomeruli (Fig. 2D, 2E) was alleviated in both BXD2-*Il17ra*$^{-/-}$ and BXD2-*Il21*$^{-/-}$ mice. Splenomegaly, which is a key autoimmune feature of BXD2-WT mice, was also reduced in both BXD2-*Il17ra*$^{-/-}$ and

BXD2-*Il21*$^{-/-}$ mice (Supplementary Fig. 2A, 2B). The frequency of GC B cells (Fas^{+}PNA^{+}CD19^{+} cells) was significantly lower in BXD2-*Il17ra*$^{-/-}$ and BXD2-*Il21*$^{-/-}$ mice than inBXD2-WT mice (Fig. 2F). Defective formation of GCs in BXD2-*Il17ra*$^{-/-}$ and BXD2-*Il21*$^{-/-}$ mice was apparent by confocal imaging analysis (Fig. 2G) and quantitation of the fractional area of PNA^{+} B cells in each IgM^{+} spleen follicle by ImageJ analysis (Fig. 2H). These data indicated that both IL-17RA and IL-21 are required for optimal GC responses and autoimmune disease development in BXD2 mice.

High numbers of functional CXCR5^{+}ICOS^{+} T_{FH} cells in BXD2-*Il17ra*$^{-/-}$ mice

IL-21 is important for the development of T_{FH} (21, 22), especially in chronic autoimmune response (15), whereas IL-17 is not required for the development of T_{FH} cells in normal mice (22). The total CD4^{+} T-cell counts in the spleens of BXD2-*Il21*$^{-/-}$ and BXD2-*Il17ra*$^{-/-}$ mice were lower than in BXD2-WT mice (Supplementary Fig. 2C). There were significantly fewer CXCR5^{+}ICOS^{+} T_{FH} cells in the spleens of BXD2-*Il21*$^{-/-}$ mice than in BXD2-WT mice (Fig. 3A, 3B, Supplementary Fig. 2D, 2E). The deficiency in IL-21, however, also resulted in a reduction in the frequency of IL-17^{+} CXCR5^{+}ICOS^{+} CD4^{+} T cells (Fig. 3C), which is consistent with the report that IL-21 can act to promote the formation of T_{H}-17 cells (42, 43).

Surprisingly, the frequency of CXCR5^{+}ICOS^{+} T_{FH} cells was significantly higher in the spleens of BXD2-*Il17ra*$^{-/-}$ mice than in BXD2-WT mice, which resulted in an equivalent cell count for this subset in both strains of mice (Fig. 3A, 3B and Supplementary Fig. 2D, 2E). The frequency of IL-21^{+} cells within the CXCR5^{+}ICOS^{+} CD4 T subset from BXD2-*Il17ra*$^{-/-}$ mice was equivalent to that in the BXD2-WT mice, whereas the frequency of IL-17-expressing cells was significantly higher (Fig. 3C). The expression of CD28, CD40L, CD62L, CD44, and IL-21R was similar in CXCR5^{+}ICOS^{+} T_{FH} cells from BXD2-WT and BXD2-*Il17ra*$^{-/-}$ mice, although the expression intensity of PD-1 was slightly, but not significantly, lower (Fig. 3D, Supplementary Fig. 2F).

To test the B-cell helper function of CXCR5^{+}ICOS^{+} CD4^{+} T cells from BXD2-*Il17ra*$^{-/-}$ mice, we co-cultured anti-CD3- plus anti-CD28-stimulated CXCR5^{+}ICOS^{+} T_{FH} cells and other CD4 T subsets based on CXCR5 and ICOS expression from either BXD2-WT or BXD2-*Il17ra*$^{-/-}$ mice with B cells from BXD2-WT mice. The ability of CXCR5^{+}ICOS^{+} CD4 T cells from BXD2-*Il17ra*$^{-/-}$ to promote B cell activation and IgG secretion was equivalent to those from BXD2-WT mice (Fig. 3E, upper, 3F). The ability of CXCR5^{+}ICOS^{+} CD4 T cells from both groups to promote IgG secretion was greater compared with other subsets of CD4 T cells, supporting the role of CXCR5^{+}ICOS^{+} CD4 T cells as the T_{FH} subset (Fig.3F). The proliferative response of CXCR5^{+}ICOS^{+} CD4^{+} T cells from BXD2-*Il17ra*$^{-/-}$ mice to anti-CD3 plus anti-CD28 stimulation was even higher than those from BXD2-WT mice (Fig. 3E, lower). Thus, despite the dramatically reduced development of spontaneous GCs in the BXD2-*Il17ra*$^{-/-}$ mice, the numbers of T_{FH} cells from these mice were not reduced, and these cells exhibited equivalent ability, compared to those from WT mice, to support the activation and IgG secretion of B cells *in vitro*.

Mislocation and reduced contact of T_{FH} cells with B cells in BXD2-*Il17ra*$^{-/-}$ mice

Confocal imaging analysis confirmed that, in the spleen follicles of BXD2-WT mice, the majority of CXCR5^{+} CD4^{+} T cells were localized in the LZ of the PNA^{+} GC area (Fig. 4A, left panels). Although intact white pulp follicles were found in the spleens of BXD2-*Il21*$^{-/-}$ mice, PNA^{+} GC structures could not be identified, and almost no CXCR5^{+} T_{FH} cells were present (Fig. 4A, right panels). By contrast, marked mis-localization of the CXCR5^{+} CD4^{+} T cells was apparent in the spleens of BXD2-*Il17ra*$^{-/-}$ mice. In these mice, many CXCR5^{+}

$CD4^+$ T cells were located outside the PNA^+ GC area and were not in immediate contact with PNA^+ GC B cells (Fig. 4A, middle panels).

To determine whether IL-17RA signaling is required for localization of T_{FH} in GC LZ, we neutralized endogenous IL-17 in WT BXD2 mice by administration of AdIL-17R:Fc. Following such treatment, there was a dramatic reduction in the localization of $CXCR5^+$ $CD4^+$ T cells to the GC LZ, and the majority of these cells were not in close contact with PNA^+ GC B cells (Fig. 4B, right). By contrast, the frequency and location of $CXCR5^+$ CD4 T cells in spleens of control AdLacZ-treated BXD2 mice were similar to those observed in untreated BXD2 mice, with the majority of these cells found in the LZ of the GCs (Fig. 4B, left). Consistent with our previous results (25), the size, weight, and cellularity of the spleen and the numbers of autoantibody-producing B cells were significantly reduced in mice treated with AdIL-17R:Fc, compared with mice treated with AdLacZ (data not shown). These results suggest that neutralization of IL-17 also disrupted the interaction of T_{FH} and GC B cells and perturbed the generation of autoantibody-producing B cells.

We next determined whether mis-location of T_{FH} cells was associated with loss of $CD4^+$ T–B cell conjugate formation in the spleens of BXD2-*Il17ra*$^{-/-}$ mice. A significantly higher percentage of B cell–CD4 T cell doublets was isolated from the spleens of BXD2-WT mice than of B6 mice (Fig. 4C upper panel and Fig. 4D) and the frequency of $CXCR5^+ICOS^+$ T_{FH} and $CXCR5^-ICOS^+$ CD4 T cells in the disassociated conjugates was higher in BXD2-WT mice than in B6 or BXD2-*Il21*$^{-/-}$ mice (Fig. 4C, lower panel and Fig. 4E). Interestingly, although there was an increased frequency of $CXCR5^+ICOS^+$ T_{FH} and $CXCR5^-ICOS^+$ CD4 T cells in the spleens of BXD2-*Il17ra*$^{-/-}$ mice, the frequency of these CD4 T cells forming conjugates with B cells was lower in BXD2-*Il17ra*$^{-/-}$ than in BXD2 mice (Fig. 4C, lower panel and Fig. 4E). These results indicate that T_{FH} cells in BXD2-*Il17ra*$^{-/-}$ mice were unable to locate to the GC LZ and that their ability to interact with B cells was compromised.

IL-17 upregulates RGS16 to mediate T_{FH} location in GC LZ

It has been reported that upregulation of RGS16 is associated with a desensitization of both B cells and $CD4^+$ T cells to CXCL12 and CXCL13 migratory cues (39, 44), thereby prolonging retention of both cells in the GC for efficient interaction. IL-17 can induce upregulation of RGS16 proteins in B cells, resulting in migration arrest (31). We investigated the association between IL-17 signaling and RGS16 expression in $CD4^+$ T cells. IL-17 stimulation of $CD4^+$ T cells isolated from the spleens of BXD2 mice resulted in a significant increase in RGS16 at both the mRNA (Fig. 5A) and protein levels (Fig. 5B). Analysis of IL-17 modulation of the T_{FH} chemotactic response to CXCL13 showed that pretreatment with IL-17 inhibited CXCL13-induced migration of T_{FH} cells from BXD2-WT mice in response to CXCL13 in the transwell assay (Fig. 5C). A similar result was found in $CXCR5^+ICOS^-$ CD4 T cells that also expressed both CXCR5 and IL-17RA (data not shown), suggesting that the migration desensitizing effect of IL-17 is not limited to $CXCR5^+ICOS^+$ T_{FH} cells. In contrast, pretreatment with IL-17 did not inhibit migration of T_{FH} from BXD2-*Rgs16*$^{-/-}$ mice (Fig. 5C). The possibility that T_{FH} cells from BXD2-*Rgs16*$^{-/-}$ mice expressed lower levels of IL-17RA compared with T_{FH} cells from BXD2-WT mice was ruled out by FACS analysis, which showed an equivalent intensity of IL-17RA (Supplementary Fig. 3A). These results suggest that RGS16 is involved in the migration arrest of T_{FH} cells stimulated by IL-17.

To further determine the function of IL-17-induced upregulation of RGS16 in the localization of T_{FH} *in vivo*, we performed confocal imaging analysis. These studies revealed that RGS16 was highly expressed by cells in spleen follicles, including CD4 T cells, in the GC LZ of BXD2-WT mice but not in BXD2-*Il17ra*$^{-/-}$ mice (Fig. 5D, upper panels).

Moreover, localization of RGS16$^+$ CD4 T cells in GC LZ mirrored that of CXCR5$^+$ CD4 T cells in the GC LZ in the spleens of BXD2 mice (Fig. 5D, lower left). By contrast, in BXD2-*Il17ra*$^{-/-}$ mice, few RGS16$^+$ cells were detected in spleen follicles, and this was associated with fewer CXCR5$^+$ CD4 T cells localized in the GC LZ (Fig. 5D, lower right). We also observed reduced numbers of CXCR5$^+$ CD4 T cells in the spleen GC LZ of BXD2-*Rgs16*$^{-/-}$ (Fig. 5E, right) compared with BXD2-WT mice (Fig. 5E, left). FACS analysis revealed a lower frequency of T_{FH} cells in the spleens of BXD2-*Rgs16*$^{-/-}$ mice than in the spleens of BXD2-WT mice (Supplementary Fig. 3B), and confocal imaging demonstrated that the size of the GCs in the spleens of BXD2-*Rgs16*$^{-/-}$ mice was also smaller than the size of the GCs formed in BXD2 mice (Fig. 5E). Analysis of T cell–B cell conjugates further showed that there was reduced *in vivo* formation of CD4 T cell–B cell conjugates (Fig. 5F), with a lower frequency of CXCR5$^+$ICOS$^+$ CD4 T and CXCR5$^-$ICOS$^+$ CD4 T cells in the conjugates isolated from the spleens of BXD2-*Rgs16*$^{-/-}$ compared with those isolated from BXD2 mice (Fig. 5G, Supplementary Fig. 3C). Collectively, these results suggest that T_{FH} cells stimulated by IL-17 increased expression of a desensitizing regulator of chemotaxis, RGS16, resulting in migration arrest in the splenic GC LZ of BXD2 mice.

IL-17 acts directly on effector CD4 T cells to promote the GC response

We previously showed that IL-17 acts through the canonical NF-κB pathway to upregulate RGS16 in B cells, thereby modulating B-cell migration responses (31). To rule out the possibility that the IL-17-induced stabilization of T_{FH} cells in the GCs is secondary to its effects on B cells, effector CD4 T cells (CD62L$^{-/lo}$) from BXD2-WT and BXD2-*Rgs16*$^{-/-}$ mice were adoptively transferred into BXD2-*Il17ra*$^{-/-}$ mice. This strategy enabled us to discriminate between IL-17RA$^+$RGS16$^+$ and IL-17RA$^+$RGS16$^-$ T_{FH} cells in an IL-17^{hi} but IL-17RA-deficient microenvironment. Six days following transfer, it was apparent that donor effector CD4$^+$ T cells from BXD2-WT mice caused an increased percentage of Fas$^+$GL7$^+$GC B cells and splenomegaly in BXD2-*Il17ra*$^{-/-}$ recipients. By contrast, donor cells from BXD2-*Rgs16*$^{-/-}$ mice did not lead to significant changes in these phenotypes in the BXD2-*Il17ra*$^{-/-}$ recipients (Fig. 6A, Supplementary Fig. 4A). ELISPOT analysis of autoantibody-producing cells on day 21 also indicated that BXD2-WT, but not BXD2-*Rgs16*$^{-/-}$, donor cells promoted autoantibody production associated with dramatically elevated numbers of autoantibody-forming B cells in BXD2-*Il17ra*$^{-/-}$ recipients (Fig. 6B, Supplementary Fig. 4B).

Analysis of conjugate formation further revealed that donor IL-17RA$^+$ CD4$^+$ T cells and CXCR5$^+$ICOS$^+$ T_{FH} cells from BXD2-WT mice had a significantly enhanced ability to form conjugates with recipient B cells compared with the same population of CD4$^+$ T cells from either BXD2-*Rgs16*$^{-/-}$ donors or from endogenous recipient BXD2-*Il17ra*$^{-/-}$ cells (Fig. 6C, Supplementary Fig. 4C). Real-time RT-PCR showed that, on day 6 post-transfer of BXD2-WT effector CD4$^+$ T cells, there was higher expression of *Rgs16* in conjugated donor IL-17RA$^+$ CD4$^+$ T cells than in singlet donor cells and in recipient IL-17RA CD4$^+$ T cells (Fig. 6D). These results further indicate that intact RGS16 in the IL-17RA$^+$ CD4$^+$ T effector cells is needed to promote the formation of spontaneous GCs, even in an environment where all other cells are IL-17RA-deficient.

IL-17RA regulates T_{FH} development and function during a T-dependent (TD) response in normal B6 mice

It is unknown whether IL-17RA-IL-17 signaling affects T_{FH} in a similar pattern in the TD response in non-autoimmune mice. To address this, we analyzed the effect of IL-17 on CD4 T cells and T_{FH} cells in normal B6 mice. CXCR5$^+$ICOS$^+$ T_{FH} cells from B6 expressed the highest level of IL-17RA followed by CXCR5$^+$ICOS$^-$ CD4 T subset, whereas, the other CD4 T subsets expressed low levels of IL-17RA (Fig. 7A). IL-17 stimulation of CD4$^+$ T

cells isolated from the spleens of B6mice resulted in a significant increase in *Rgs16* at the 4 hour time point (Fig. 7B) and also inhibited migration of CD4 T cells in response to CXCL13 in the transwell assay (Fig. 7C). To further investigate T_{FH} response in B6-*Il17ra*$^{-/-}$ mice during a TD response, B6-*Il17ra*$^{-/-}$ mice and WT B6 mice were immunized with NP (21)-CGG and sacrificed on day 6, 9 and 12. The results indicate that the frequency of T_{FH} peaked on day 9, and began to decrease by day 12 after NP-CGG immunization. The T_{FH} frequency was synchronized with that of anti-NP IgG antibody level in sera, whereas the GC B population peaked on day 12. On day 9, the frequency of CXCR5^{+}ICOS^{+} T_{FH} was approximately two folds higher in B6-*Il17ra*$^{-/-}$ mice, compared with WT B6 (Fig. 7D, left). Although IL-21 production was comparable, production of IL-17 by CXCR5^{+}ICOS^{+} T_{FH} cells was significantly increased in B6-*Il17ra*$^{-/-}$ mice, compared with WT B6 (Fig. 7D, middle). The frequency of GC B cells was, however, higher in WT compared with B6-*Il17ra*$^{-/-}$ mice (Fig. 7D, right), which is consistent with the lower number of high affinity anti-NP IgG antibody producing B cells detected by ELISPOT in B6-*Il17ra*$^{-/-}$ mice (Fig. 7E). Confocal image analysis showed that, on day 9, CXCR5^{+} CD4 T cells could be localized in the LZ of the GCs in the spleen of WT B6 mice (Fig. 7F, left, yellow color). By contrast, although many CXCR5^{+} CD4 T cells were identified in the spleen of B6-*Il17ra*$^{-/-}$ mice, these CXCR5^{+} CD4 T cells were not localized to the LZ of the smaller GCs found in these mice (Fig. 7F, right, yellow color). These results indicate that, even in normal mice, IL-17RA-IL-17 signaling can regulate T_{FH} cell localization in GC LZ potentially via upregulation of *Rgs16* in T_{FH} cells to promote GC development and high affinity antibody production.

Discussion

Analysis of the CD4^{+} T subpopulations in the spleens of BXD2 mice provided several unique insights into the regulation of T_{FH} cell function. First, we found that the majority of cells that expressed the high levels of CXCR5 typical of T_{FH} cells also expressed high levels of IL-17RA, and thus were potentially capable of responding to IL-17. Second, our data suggest that in BXD2 mice, a subset of CD4^{+} T cells with phenotypic characteristics of T_{FH} cells was capable of producing IL-17 rather than IL-21. CD4^{+} T cells with the characteristics of T_H17 cells (CXCR5^{-}ICOS^{+}) were also present. Third, the loss of IL-17RA affected the stabilization of T_{FH} in GC LZ. These results together suggest that IL-17 plays an essential role in stabilizing T_{FH} location and close contact with B cells in GCs. IL-17 thus complements the effects of IL-21, and both cytokines are needed for pathogenic GC development in BXD2 mice, as loss of either cytokine dramatically abrogated this response.

The parameters that should be used to define T_{FH} cells are currently a matter of debate. Moreover, the relationship of T_{FH} cells to other CD4^{+} T cell populations, including T_H17 cells, is unclear and it has been suggested that there is a considerable degree of plasticity (19, 45). A recent study shows that, in human tonsils, while IL-21 was the major cytokine produced by CXCR5^{hi} T_{FH} cells, IL-17 was produced mainly by CXCR5$^{lo/-}$ CD4 T cells (24). However, in autoimmune BXD2 mouse spleen, IL-17 and IL-21 could be produced by two separate subsets of CXCR5^{+}ICOS^{+} T_{FH} cells and IL-17 could be further identified in CXCR5^{-}ICOS^{+} CD4 T cells. Interestingly, these IL-17 producing T_{FH} cells are different from the conventional T_H17 by their surface phenotype and location.

In agreement with previous studies (22), we found that IL-21, but not IL-17, was important for the proper development of T_{FH} cells in this autoimmune mouse model. Although there were almost no GCs in BXD2-*Il21*$^{-/-}$ mice, the deficiency of IL-21 did not appear to perturb the structure of the follicles in the spleens in that there was a normal distribution of CD4^{+} T cells surrounded by IgM^{+} B cells. Development of T_H17 cells was significantly reduced in BXD2-*Il21*$^{-/-}$ mice, which is also consistent with the previous finding that IL-21 exhibits a

unique effect in promoting T_H17 differentiation (42, 43). In contrast, the frequency and total numbers of T_{FH} cells were not reduced by lack of IL-17RA expression in the BXD2-*Il17ra*$^{-/-}$ mice as well as in NP-CGG immunized B6-*Il17ra*$^{-/-}$ mice. The proliferative response of T_{FH} cells from BXD2-*Il17ra*$^{-/-}$ and their ability to induce B cell proliferation and IgG secretion *in vitro* were also intact. Surprisingly, the sera titers of IgG autoantibodies were similar in the BXD2-*Il17ra*$^{-/-}$ and BXD2-*Il21*$^{-/-}$ mice. Confocal imaging analysis confirmed our previous report (28) of a dissipation of B cells in the follicles of the BXD2-*Il17ra*$^{-/-}$ mice and further indicated that the majority of CXCR5^{+} T_{FH} cells were not localized in the GC LZ. The present study suggests that IL-21 acts at an early checkpoint to cue the development of T_{FH}, whereas IL-17 acts at a later checkpoint at the LZ to enable prolonged interaction of differentiated T_{FH} to help GC B cell maturation.

Under optimal conditions for generating antibody-forming B cells, both GC B cells and T_{FH} exhibit a tendency to migrate towards the same LZ compartment, thereby enhancing their opportunity for cognate interactions (46). Although recruitment to the GC LZ is enabled by CXCL13, special migration “stop” signaling events are required to induce conjugate formation. Prolonged interactions between CD4 T cells and APCs have been shown to enable the generation of autoreactive T cells and such immobilization is associated with TCR signals and can affect the future activation fate of T cells (47). Similarly, stable interaction between CD4 T cells and cognate B cells mediated by SAP is another intrinsic mechanism to retain CD4 T cells in a nascent germinal center for sustain GC reaction (48). The present study, however, suggests that IL-17 is an extrinsic stop signal that it acts on post-differentiated IL-17RA^{+} T_{FH} as a “braking trigger” to enable its interaction with responder B cells in the LZ niche. This unique property is especially important for a GC response for which T-cell help is proposed to be the limiting factor in the establishment of stable conjugates (49). This braking effect of IL-17 in BXD2 mice may preferentially occur in the LZ because IL-17^{+} CD4 cells are mainly located in this region. It has been reported that GC CD4^{+} T cells utilize the RGS13 and RGS16 signaling proteins to modulate their trafficking and that GC B cells utilize RGS1, RGS13, and RGS16 during CXCL12/13-induced formation of GCs (39, 44). Here we show that, in the BXD2 mouse, RGS16 is responsible for the IL-17-mediated migration arrest of T_{FH} cells in the GC LZ, providing the necessary cell anchorage for cognate B–T cell interactions and GC development. We found that IL-17 stimulated the expression of RGS16 in CD4 T cells at both the transcriptional and protein levels and that IL-17 stimulation inhibited CXCL13-mediated chemotaxis of T_{FH} cells isolated from RGS16^{+} BXD2 mice but not BXD2-*Rgs16*$^{-/-}$ mice. The lack of aggregating T_{FH} cells in GC LZ in the spleen of BXD2-*Il17ra*$^{-/-}$ mice was recapitulated in BXD2-*Rgs16*$^{-/-}$ mice. Furthermore, T_{FH} cells from BXD2-WT, but not BXD2-*Rgs16*$^{-/-}$ mice that were adoptively transferred into BXD2-*Il17ra*$^{-/-}$, formed more conjugates with B cells and supported the resumption of GC formation in the recipients. These observations provide further evidence that IL-17-induced upregulation of RGS16 plays a dominant role in the proper localization of T_{FH} cells in GC LZ. Under these experimental conditions, the B cells as well as all other host cells were IL-17RA-deficient. Together with our previous findings concerning the effects of IL-17 on B cells (28, 31), the current results suggest that T_{FH}–B conjugate formation in GCs can be regulated by modification of the chemotactic responses of either cell type at the post-receptor level.

Why is regulation of the location of T_{FH} cells and their prolonged interactions with GC B cells important for development of highly pathogenic autoantibodies in BXD2 mice that can passively transfer autoimmunity (30)? T_{FH} cells located within GCs drive positive selection of B cells that have acquired high-affinity receptors (3, 4). The cognate contact between T_{FH} and GC B cells, mediated by a series of cell-surface co-stimulator interactions, such as CD28–CD86, ICOS–ICOSL, and CD40L–CD40, is required for class-switch recombination (CSR) and somatic hypermutation (SHM) (25). New evidence further suggests that the

ability to induce SHM plays an important role in the survival of self-reactive B cells in the GC (50). The present results indicate that perturbation of IL-17 signaling, either acutely by AdIL-17R:Fc or chronically by *Il17ra*$^{-/-}$, disrupts T_{FH}–B interactions and abrogates the generation of autoantibody-forming B cells in BXD2 mice. As a soluble mediator, IL-17 potentially defies TCR specificity and unselectively arrests all IL-17R^{+} T_{FH} cells in the LZ niche, enhancing the opportunity of cognate interactions of T_{FH}–B cells to drive the development of pathogenic polyreactive autoantibody-forming B cells in BXD2 mice (28, 30). Because the T_{FH} phenotype and numbers are normal in BXD2-*Il17ra*$^{-/-}$ mice, the present study further suggests that T_{FH} cell differentiation can be dissociated from GCs but that their anatomical location in the GC LZ is indispensable for their function in supporting autoreactive GC B cell maturation.

Supplementary Material

Refer to Web version on PubMed Central for supplementary material.

Acknowledgments

We thank Drs. Jay Kolls (University of Pittsburgh) and Paul Robbins (University of Pittsburgh) for providing AdIL-17 and AdLacZ. We thank Amgen Inc. (Thousand Oaks, CA) and the Mutant Mice Regional Resource Center (Davis, CA) for providing IL-17RA and IL-21-deficient mice, respectively. We thank Drs. Fiona Hunter and Paul Todd for review of the manuscript, Dr. Chander Raman for critical discussion, and Ms. Karen Beeching for excellent secretarial assistance. Flow cytometry and confocal imaging data acquisition were carried out at the UAB Comprehensive Flow Cytometry Core (P30 AR048311 and P30 AI027767) and UAB Analytic Imaging and Immunoreagents Core (P30 AR048311), respectively.

References

1. Linterman MA, Liston A, Vinuesa CG. T-follicular helper cell differentiation and the co-option of this pathway by non-helper cells. Immunol Rev. 2012; 247:143–159. [PubMed: 22500838]
2. Shlomchik MJ, Weisel F. Germinal center selection and the development of memory B and plasma cells. Immunol Rev. 2012; 247:52–63. [PubMed: 22500831]
3. Crotty S. The 1-1-1 fallacy. Immunol Rev. 2012; 247:133–142. [PubMed: 22500837]
4. Ma CS, Deenick EK, Batten M, Tangye SG. The origins, function, and regulation of T follicular helper cells. The Journal of experimental medicine. 2012; 209:1241–1253. [PubMed: 22753927]
5. Linterman MA, Rigby RJ, Wong RK, Yu D, Brink R, Cannons JL, Schwartzberg PL, Cook MC, Walters GD, Vinuesa CG. Follicular helper T cells are required for systemic autoimmunity. The Journal of experimental medicine. 2009; 206:561–576. [PubMed: 19221396]
6. Craft JE. Follicular helper T cells in immunity and systemic autoimmunity. Nat Rev Rheumatol. 2012; 8:337–347. [PubMed: 22549246]
7. Vinuesa CG, Sanz I, Cook MC. Dysregulation of germinal centres in autoimmune disease. Nat Rev Immunol. 2009; 9:845–857. [PubMed: 19935804]
8. Lee SK, Silva DG, Martin JL, Pratama A, Hu X, Chang PP, Walters G, Vinuesa CG. Interferon-gamma Excess Leads to Pathogenic Accumulation of Follicular Helper T Cells and Germinal Centers. Immunity. 2012; 37:880–892. [PubMed: 23159227]
9. Sweet RA, Lee SK, Vinuesa CG. Developing connections amongst key cytokines and dysregulated germinal centers in autoimmunity. Curr Opin Immunol. 2012
10. Simpson N, Gatenby PA, Wilson A, Malik S, Fulcher DA, Tangye SG, Manku H, Vyse TJ, Roncador G, Huttley GA, Goodnow CC, Vinuesa CG, Cook MC. Expansion of circulating T cells resembling follicular helper T cells is a fixed phenotype that identifies a subset of severe systemic lupus erythematosus. Arthritis Rheum. 2010; 62:234–244. [PubMed: 20039395]
11. Ma J, Zhu C, Ma B, Tian J, Baidoo SE, Mao C, Wu W, Chen J, Tong J, Yang M, Jiao Z, Xu H, Lu L, Wang S. Increased frequency of circulating follicular helper T cells in patients with rheumatoid arthritis. Clinical & developmental immunology. 2012; 2012:827480. [PubMed: 22649468]

12. Feng X, Wang D, Chen J, Lu L, Hua B, Li X, Tsao BP, Sun L. Inhibition of aberrant circulating Tfh cell proportions by corticosteroids in patients with systemic lupus erythematosus. PloS one. 2012; 7:e51982. [PubMed: 23284839]

13. Lu KT, Kanno Y, Cannons JL, Handon R, Bible P, Elkahloun AG, Anderson SM, Wei L, Sun H, O'Shea JJ, Schwartzberg PL. Functional and epigenetic studies reveal multistep differentiation and plasticity of in vitro-generated and in vivo-derived follicular T helper cells. Immunity. 2011; 35:622–632. [PubMed: 22018472]

14. Terrier B, Costedoat-Chalumeau N, Garrido M, Geri G, Rosenzwajg M, Musset L, Klatzmann D, Saadoun D, Cacoub P. Interleukin 21 correlates with T cell and B cell subset alterations in systemic lupus erythematosus. J Rheumatol. 2012; 39:1819–1828. [PubMed: 22859347]

15. Bubier JA, Sproule TJ, Foreman O, Spolski R, Shaffer DJ, Morse HC 3rd, Leonard WJ, Roopenian DC. A critical role for IL-21 receptor signaling in the pathogenesis of systemic lupus erythematosus in BXSB-Yaa mice. Proc Natl Acad Sci U S A. 2009; 106:1518–1523. [PubMed: 19164519]

16. Zotos D, Coquet JM, Zhang Y, Light A, D'Costa K, Kallies A, Corcoran LM, Godfrey DI, Toellner KM, Smyth MJ, Nutt SL, Tarlinton DM. IL-21 regulates germinal center B cell differentiation and proliferation through a B cell-intrinsic mechanism. The Journal of experimental medicine. 2010; 207:365–378. [PubMed: 20142430]

17. Poholek AC, Hansen K, Hernandez SG, Eto D, Chandele A, Weinstein JS, Dong X, Odegard JM, Kaech SM, Dent AL, Crotty S, Craft J. In vivo regulation of Bcl6 and T follicular helper cell development. Journal of immunology. 2010; 185:313–326.

18. Eto D, Lao C, DiToro D, Barnett B, Escobar TC, Kageyama R, Yusuf I, Crotty S. IL-21 and IL-6 are critical for different aspects of B cell immunity and redundantly induce optimal follicular helper CD4 T cell (Tfh) differentiation. PloS one. 2011; 6:e17739. [PubMed: 21423809]

19. Luthje K, Kallies A, Shimohakamada Y, GT TB, Light A, Tarlinton DM, Nutt SL. The development and fate of follicular helper T cells defined by an IL-21 reporter mouse. Nat Immunol. 2012; 13:491–498. [PubMed: 22466669]

20. Yu D, Rao S, Tsai LM, Lee SK, He Y, Sutcliffe EL, Srivastava M, Linterman M, Zheng L, Simpson N, Ellyard JI, Parish IA, Ma CS, Li QJ, Parish CR, Mackay CR, Vinuesa CG. The transcriptional repressor Bcl-6 directs T follicular helper cell lineage commitment. Immunity. 2009; 31:457–468. [PubMed: 19631565]

21. Vogelzang A, McGuire HM, Yu D, Sprent J, Mackay CR, King C. A fundamental role for interleukin-21 in the generation of T follicular helper cells. Immunity. 2008; 29:127–137. [PubMed: 18602282]

22. Nurieva RI, Chung Y, Hwang D, Yang XO, Kang HS, Ma L, Wang YH, Watowich SS, Jetten AM, Tian Q, Dong C. Generation of T follicular helper cells is mediated by interleukin-21 but independent of T helper 1, 2, or 17 cell lineages. Immunity. 2008; 29:138–149. [PubMed: 18599325]

23. Johnston RJ, Poholek AC, DiToro D, Yusuf I, Eto D, Barnett B, Dent AL, Craft J, Crotty S. Bcl6 and Blimp-1 are reciprocal and antagonistic regulators of T follicular helper cell differentiation. Science. 2009; 325:1006–1010. [PubMed: 19608860]

24. Kroenke MA, Eto D, Locci M, Cho M, Davidson T, Haddad EK, Crotty S. Bcl6 and Maf cooperate to instruct human follicular helper CD4 T cell differentiation. Journal of immunology. 2012; 188:3734–3744.

25. Fazilleau N, Mark L, McHeyzer-Williams LJ, McHeyzer-Williams MG. Follicular helper T cells: lineage and location. Immunity. 2009; 30:324–335. [PubMed: 19303387]

26. Weinstein JS, Hernandez SG, Craft J. T cells that promote B-Cell maturation in systemic autoimmunity. Immunol Rev. 2012; 247:160–171. [PubMed: 22500839]

27. Wong CK, Lit LC, Tam LS, Li EK, Wong PT, Lam CW. Hyperproduction of IL-23 and IL-17 in patients with systemic lupus erythematosus: implications for Th17-mediated inflammation in auto-immunity. Clin Immunol. 2008; 127:385–393. [PubMed: 18373953]

28. Hsu HC, Yang P, Wang J, Wu Q, Myers R, Chen J, Yi J, Guentert T, Tousson A, Stanus AL, Le TV, Lorenz RG, Xu H, Kolls JK, Carter RH, Chaplin DD, Williams RW, Mountz JD. Interleukin

17-producing T helper cells and interleukin 17 orchestrate autoreactive germinal center development in autoimmune BXD2 mice. Nat Immunol. 2008; 9:166–175. [PubMed: 18157131]

29. Mitsdoerffer M, Lee Y, Jager A, Kim HJ, Korn T, Kolls JK, Cantor H, Bettelli E, Kuchroo VK. Proinflammatory T helper type 17 cells are effective B-cell helpers. Proc Natl Acad Sci U S A. 2010; 107:14292–14297. [PubMed: 20660725]
30. Hsu HC, Zhou T, Kim H, Barnes S, Yang P, Wu Q, Zhou J, Freeman BA, Luo M, Mountz JD. Production of a novel class of polyreactive pathogenic autoantibodies in BXD2 mice causes glomerulonephritis and arthritis. Arthritis Rheum. 2006; 54:343–355. [PubMed: 16385526]
31. Xie S, Li J, Wang JH, Wu Q, Yang P, Hsu HC, Smythies LE, Mountz JD. IL-17 activates the canonical NF-kappaB signaling pathway in autoimmune B cells of BXD2 mice to upregulate the expression of regulators of G-protein signaling 16. Journal of immunology. 2010; 184:2289–2296.
32. Toy D, Kugler D, Wolfson M, Vanden Bos T, Gurgel J, Derry J, Tocker J, Peschon J. Cutting edge: interleukin 17 signals through a heteromeric receptor complex. Journal of immunology. 2006; 177:36–39.
33. Yao Z, Fanslow WC, Seldin MF, Rousseau AM, Painter SL, Comeau MR, Cohen JI, Spriggs MK. Herpesvirus Saimiri encodes a new cytokine, IL-17, which binds to a novel cytokine receptor. Immunity. 1995; 3:811–821. [PubMed: 8777726]
34. Cai G, Nie X, Zhang W, Wu B, Lin J, Wang H, Jiang C, Shen Q. A regulatory role for IL-10 receptor signaling in development and B cell help of T follicular helper cells in mice. Journal of immunology. 2012; 189:1294–1302.
35. Ye P, Rodriguez FH, Kanaly S, Stocking KL, Schurr J, Schwarzenberger P, Oliver P, Huang W, Zhang P, Zhang J, Shellito JE, Bagby GJ, Nelson S, Charrier K, Peschon JJ, Kolls JK. Requirement of interleukin 17 receptor signaling for lung CXC chemokine and granulocyte colony-stimulating factor expression, neutrophil recruitment, and host defense. The Journal of experimental medicine. 2001; 194:519–527. [PubMed: 11514607]
36. Yi JS, Du M, Zajac AJ. A vital role for interleukin-21 in the control of a chronic viral infection. Science. 2009; 324:1572–1576. [PubMed: 19443735]
37. Reinhardt RL, Liang HE, Locksley RM. Cytokine-secreting follicular T cells shape the antibody repertoire. Nat Immunol. 2009; 10:385–393. [PubMed: 19252490]
38. Hsu HC, Yang P, Wu Q, Wang JH, Job G, Guentert T, Li J, Stockard CR, Le TV, Chaplin DD, Grizzle WE, Mountz JD. Inhibition of the catalytic function of activation-induced cytidine deaminase promotes apoptosis of germinal center B cells in BXD2 mice. Arthritis Rheum. 2011; 63:2038–2048. [PubMed: 21305519]
39. Moratz C, Harrison K, Kehrl JH. Regulation of chemokine-induced lymphocyte migration by RGS proteins. Methods Enzymol. 2004; 389:15–32. [PubMed: 15313557]
40. Mountz JD, Yang P, Wu Q, Zhou J, Tousson A, Fitzgerald A, Allen J, Wang X, Cartner S, Grizzle WE, Yi N, Lu L, Williams RW, Hsu HC. Genetic segregation of spontaneous erosive arthritis and generalized autoimmune disease in the BXD2 recombinant inbred strain of mice. Scand J Immunol. 2005; 61:128–138. [PubMed: 15683449]
41. Wang JH, Li J, Wu Q, Yang P, Pawar RD, Xie S, Timares L, Raman C, Chaplin DD, Lu L, Mountz JD, Hsu HC. Marginal zone precursor B cells as cellular agents for type I IFN-promoted antigen transport in autoimmunity. Journal of immunology. 2010; 184:442–451.
42. Zhou L, Ivanov II, Spolski R, Min R, Shenderov K, Egawa T, Levy DE, Leonard WJ, Littman DR. IL-6 programs T (H)-17 cell differentiation by promoting sequential engagement of the IL-21 and IL-23 pathways. Nat Immunol. 2007; 8:967–974. [PubMed: 17581537]
43. Korn T, Bettelli E, Gao W, Awasthi A, Jager A, Strom TB, Oukka M, Kuchroo VK. IL-21 initiates an alternative pathway to induce proinflammatory T (H)17 cells. Nature. 2007; 448:484–487. [PubMed: 17581588]
44. Estes JD, Thacker TC, Hampton DL, Kell SA, Keele BF, Palenske EA, Druey KM, Burton GF. Follicular dendritic cell regulation of CXCR4-mediated germinal center CD4 T cell migration. Journal of immunology. 2004; 173:6169–6178.
45. Spolski R, Leonard WJ. Interleukin-21: basic biology and implications for cancer and autoimmunity. Annu Rev Immunol. 2008; 26:57–79. [PubMed: 17953510]

46. Beltman JB, Allen CD, Cyster JG, de Boer RJ. B cells within germinal centers migrate preferentially from dark to light zone. Proc Natl Acad Sci U S A. 2011; 108:8755–8760. [PubMed: 21555569]

47. Fife BT, Pauken KE, Eagar TN, Obu T, Wu J, Tang Q, Azuma M, Krummel MF, Bluestone JA. Interactions between PD-1 and PD-L1 promote tolerance by blocking the TCR-induced stop signal. Nat Immunol. 2009; 10:1185–1192. [PubMed: 19783989]

48. Qi H, Cannons JL, Klauschen F, Schwartzberg PL, Germain RN. SAP-controlled T-B cell interactions underlie germinal centre formation. Nature. 2008; 455:764–769. [PubMed: 18843362]

49. Allen CD, Okada T, Tang HL, Cyster JG. Imaging of germinal center selection events during affinity maturation. Science. 2007; 315:528–531. [PubMed: 17185562]

50. Chan TD, Wood K, Hermes JR, Butt D, Jolly CJ, Basten A, Brink R. Elimination of germinal-center-derived self-reactive B cells is governed by the location and concentration of self-antigen. Immunity. 2012; 37:893–904. [PubMed: 23142780]

Abbreviations in this paper

GC	germinal center
NP-CGG	4-Hydroxy-3-nitrophenylacetyl hapten conjugated to chicken gamma globulin
LZ	light zone
PNA	peanut agglutinin
T_{FH}	follicular T helper cells
RGS	regulators of G-protein signaling

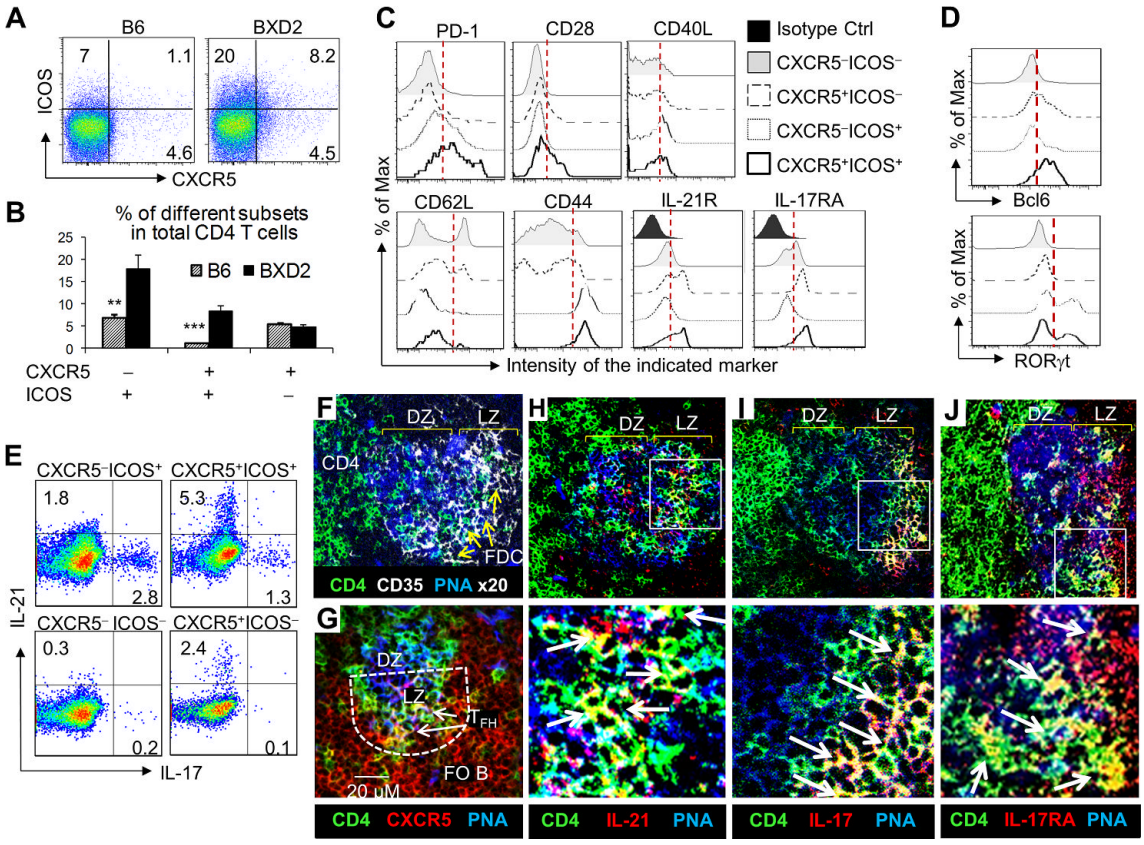

Figure 1. Increased CXCR5$^+$ICOS$^+$ T$_{FH}$cells producing IL-21 or IL-17 in spleen GCs in naïve BXD2 mice

(**A-E**) Flow cytometry analysis of CD4 T subsets based on the expression of CXCR5 and ICOS in the spleens of female 10-12-week-old mice. Cells were first gated for CD4 T cells. (**A**) Analysis of CXCR5 and ICOS. (**B**) Frequency of the indicated CD4 T subsets. (**C**) Analysis of the indicated cell surface markers or (**D**) intranuclear Bcl6 and RORγt on CD4 T subsets in BXD2 mice. Cells were gated based on the differential expression of CXCR5 and ICOS. (**E**) Analysis of intracellular IL-21 and IL-17 produced by the indicated CD4 T subsets from BXD2 mice. (**F-J**) Confocal imaging analysis of frozen spleen sections from 3-mo-old BXD2 mice. Sections were stained with fluorochrome-conjugated reagents or antibodies. Abbreviations used: FDC, follicular dendritic cell (yellow arrows, **F**); FO B, follicular B cells; DZ, dark zone; LZ, light zone. The GC LZ vicinity is marked by a white dashed line (**G**). A higher-magnification view of the boxed area is shown (**H**, **I**, **J**, lower). White arrows indicate representative CXCR5$^+$ CD4 T cells (**G**), IL-21$^+$ CD4 T cells (**H**), IL-17$^+$ CD4 T cells (**I**), or IL-17RA$^+$ CD4 T cells (**J**) in the GC LZ. Data are representative of the analysis. Numbers in dot plots indicate the percentage of cells in each quadrant (**A**,**E**). Bar graph results from (**B**) are shown as mean ± s.d.; n ≥ 5 per group; **p<0.01 and ***p<0.005 between B6 and BXD2 (**B**).

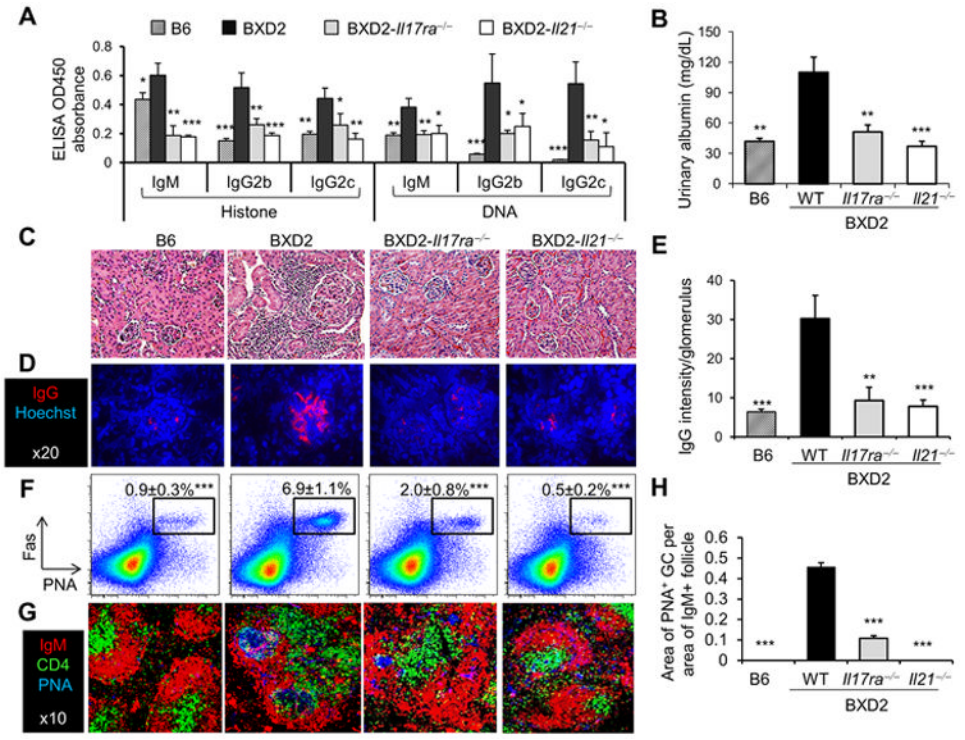

Figure 2. GC development and autoimmune disease severity were alleviated in BXD2-*Il17ra*$^{-/-}$ and BXD2-*Il21*$^{-/-}$ mice

(**A**) ELISA of IgM, IgG2b, and IgG2c autoantibodies specific for histone and DNA in the sera of 4–5-mo-old mice. (**B**) ELISA of urinary albumin in 4–5-mo-old mice. (**C**) H&E staining in paraffin-embedded kidney sections from 5-mo-old mice. Magnification, ×20. (**D**) Immunofluorescence analysis for IgG (red) deposition in glomeruli in frozen kidney sections from 5-mo-old mice. Magnification, ×20. Each image was equally magnified digitally further to show the detail structure. (**E**) ImageJ quantitation of the intensity of IgG deposition per glomerulus in frozen kidney sections from 5-mo-old mice. (**F**) Flow cytometry analysis of the percentage of PNA^{+}Fas^{+} GC B cells in the spleens of 2–3-mo-old mice. Cells were gated on CD19^{+} B cells. Numbers above the boxed region represent the frequency of PNA^{+}Fas^{+} within CD19^{+} cells (mean ± s.d.). (**G**, **H**) Confocal imaging analysis of PNA^{+} GC B cells in frozen spleen sections from 2–3-mo-old mice. (**G**) Sections were stained with anti-IgM (red), anti-CD4 (green), and PNA (blue). Magnification, ×10. (**H**) ImageJ quantitation of the area of PNA^{+} staining versus the area of each IgM^{+} spleen follicle. All data are representative or an average of n ≥ 5 female mice per group; *p < 0.05, **p < 0.01, ***p< 0.005 compared with BXD2-WT mice.

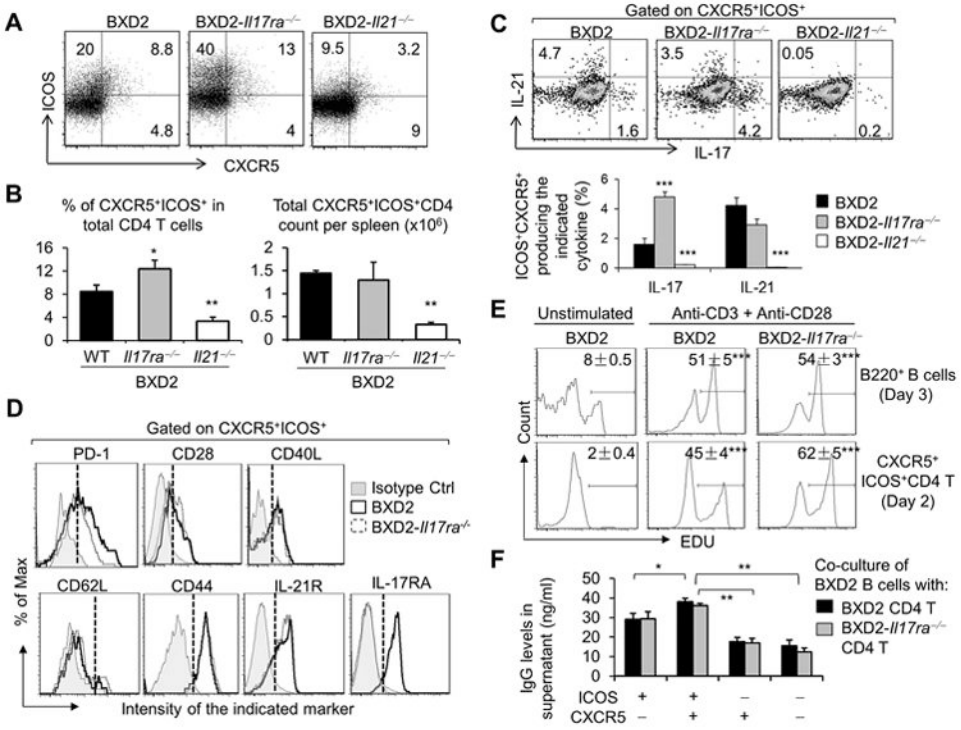

Figure 3. Increased frequency of T_{FH} cells in the spleens of BXD2-*Il17ra*$^{-/-}$ mice

Single-cell suspensions were prepared from the spleens of female 10–12-week-old mice. (**A**) Flow cytometry analysis of CXCR5 and ICOS on CD4 T cells. (**B**) Bar graph showing the frequency (left) and the total cell count of $CXCR5^+ICOS^+$ T_{FH} cells per spleen (right). (**C**) Upper: Flow cytometry analysis of intracellular IL-21 and IL-17 produced by $CXCR5^+ICOS^+$ T_{FH} cells. Cells were gated on $CD4^+$ T cells first. Lower: Quantitation of the percentage of $CXCR5^+ICOS^+$ T_{FH} that expressed either IL-17 or IL-21. (**D**) Flow cytometry analysis of the indicated cell surface markers on $CXCR5^+ICOS^+$ CD4 T cells. (**E, F)** Functional assay of T cells *in vitro*. Sorted T_{FH} cells and other CD4 T subsets based on CXCR5 and ICOS expression from BXD2-WT or *Il17ra*$^{-/-}$ mice, either unstimulated or stimulated with anti-CD3 plus anti-CD28, were co-cultured with B cells from BXD2 mice. Flow cytometry analysis of the proliferative responses indicated by EDU^+ staining was carried out on day 3 for B cells (upper) and day 2 for T cells (lower). **(F)** ELISA analysis of IgG secretion in the coculture supernatant on day 3 after subtraction of the background levels without anti-CD3 and anti-CD28 stimulation. Numbers in quadrants or above gate indicate the percentage of cells (**A**, **C**) or the mean percentage ± s.d. (**E, F**). Data are representative of the analysis of n = 5 mice per group (**A**, **C** upper panel, **D**), two independent experiments with n = 3 mice per group (**E, F**), or are the mean ± s.d. of n = 5 mice per group (**B**, **C** lower panel); *p < 0.05, **p < 0.01, ***p< 0.005 compared with BXD2-WT mice (**B**, **C**), the unstimulated group (**E**), or the $CXCR5^+ICOS^+$ CD4 T subset (**F**).

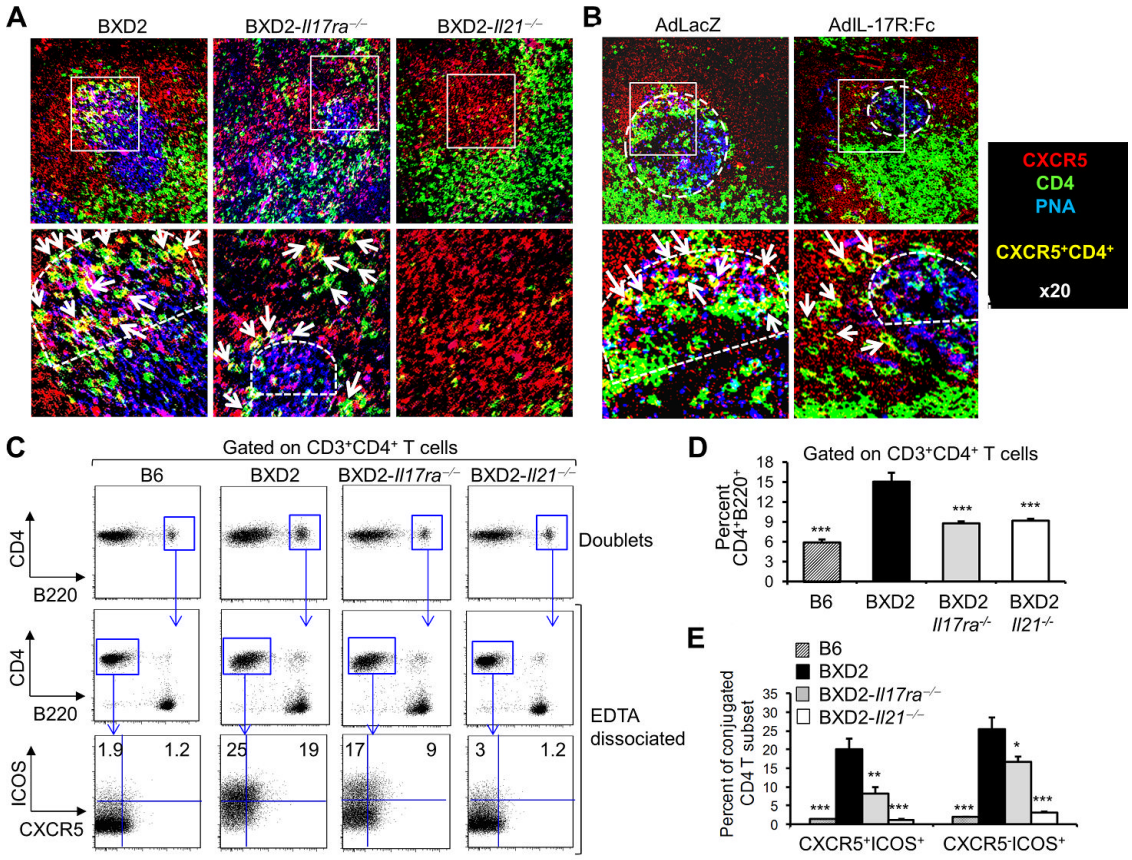

Figure 4. Abnormal localization of T_{FH} cells and defective T_{FH}–B cell conjugates in the spleens of BXD2-*Il17ra*$^{-/-}$ mice

(**A-B**) Immunofluorescence microscopy of frozen sections from spleens of naive 3-mo-old mice (**A**) or from spleens of 2.5-mo-old mice 10 days post-administration of either AdLacZ or AdIL-17R:Fc (**B**). Sections were stained with anti-CXCR5 (red), anti-CD4 (green), and PNA (blue). The GC border is marked by a white dashed line (**B**, upper), and the white rectangle regions from the upper panels were further magnified to show the distribution of $CXCR5^+$ CD4 T cells (yellow, arrows). The GC LZ vicinity is marked by a white dashed line (all lower panels). (**C-E**) Analysis of conjugates formed between $CXCR5^+ICOS^+$ CD4 T and B cells in the spleens of 3-mo-old mice. (**C**) FACS sorting of CD4–B220 cell conjugates. Upper: Cells gated on $CD3^+$ $CD4^+$ T cells prior to acquisition of $CD4^+B220^+$ doublets. Middle: Conjugated cells were dissociated with EDTA/PBS as described (37) to yield CD4 and B200 single cells. Lower: Analysis of expression of ICOS and CXCR5 within the dissociated CD4 T cells; numbers in quadrants indicate frequency. (**D**) Frequency of $CD4^+B220^+$ doublets in the $CD3^+$ $CD4^+$ T cells in each strain. (**E**) Frequency of $CXCR5^+ICOS^+$ or $CXCR5^-ICOS^+$ cells in dissociated CD4 T cells. Data are representative of the analysis of n = 5 mice per group (**A**), two independent experiments with n = 3 mice per group (**B**, **C**), or indicate mean ± s.d.;*p < 0.05, ***p< 0.005 compared with BXD2-WT mice (**D**, **E**).

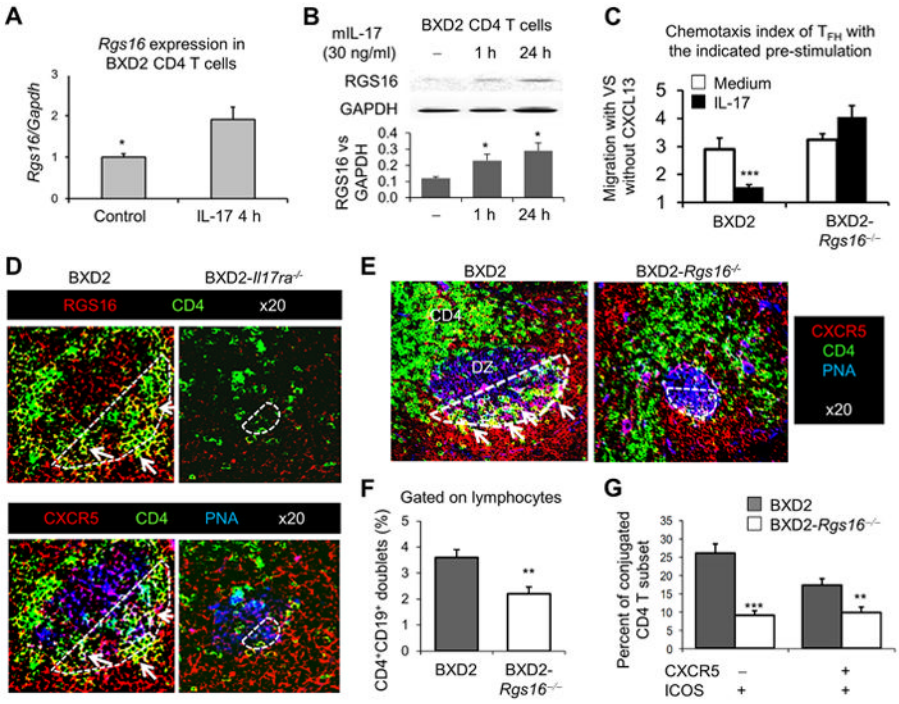

Figure 5. RGS16 is involved in IL-17-induced location of CXCR5$^+$ CD4 T cells

(**A-C**) MACS-purified CD4 T cells from spleens were cultured with/without IL-17 (30 ng/ml) *in vitro*. (**A**) qRT-PCR analysis of *Rgs16* and (**B**) western blot and ImageJ quantitation of RGS16 at the indicated times. (**C**) Chemotactic response of CXCR5$^+$ICOS$^+$ CD4 T cells. Culture medium or IL-17-pre-incubated CD4 T cells in response to CXCL13 or medium were analyzed. Migrated cells were counted and the percentage of CXCR5$^+$ICOS$^+$ T_{FH} cells was determined by flow cytometry. The chemotaxis index was calculated as previously described (39). (**D**) Immunofluorescence microscopy of frozen spleen sections of naïve mice. For both strains, the same spleen follicle is presented for each staining. Arrows indicate representative RGS16$^+$ CD4 T cells (yellow, upper) or CXCR5$^+$CD4 T cells (yellow, lower) in the GC LZ. (**E**) Immunofluorescence microscopy of frozen spleen sections showing the localization of CXCR5$^+$CD4 T cells in naïve mice. Magnification, ×20. GC LZ vicinity is marked by a white dashed line (**D**, **E**). (**F**, **G**) B cell–T cell conjugate analysis of the indicated strains. (**F**) Frequency of CD4$^+$CD19$^+$ doublets in spleen cells. (**G**) Frequency of CXCR5$^-$ICOS$^+$ or CXCR5$^+$ICOS$^+$ CD4 T cells dissociated from the CD4$^+$CD19$^+$ doublets. Data are representative of the analysis of 3–4 mice (2.5–3-mo-old) per group (**D**, **E**) or indicate mean ± s.d. of 2–3 mice per group for three repeated experiments;*$p < 0.05$, ** $p<0.01$, ***$p< 0.005$ between the groups **(A, B, C, F, G)**.

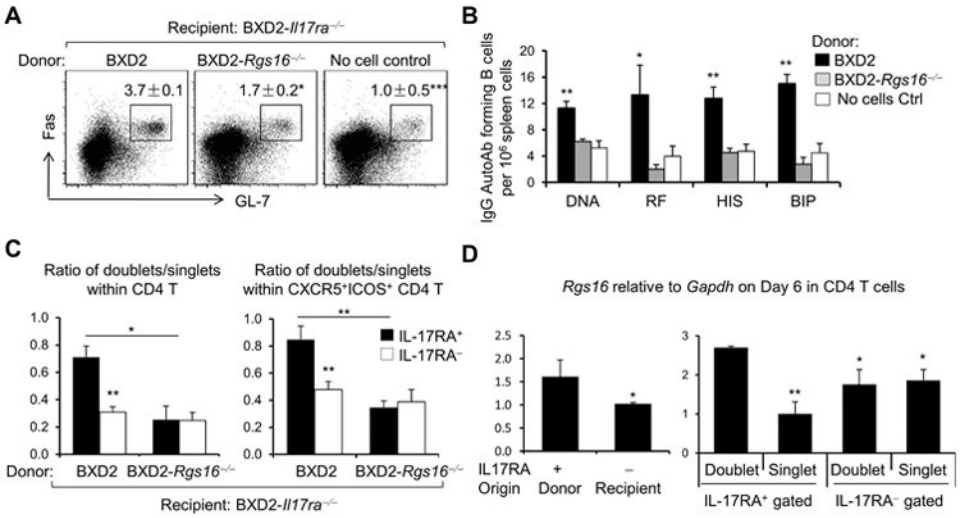

Figure 6. RGS16^{+}IL-17RA^{+}, but not RGS16^{-}IL-17RA^{+}, CD4 T cells resumed GC formation in BXD2-*Il17ra*$^{-/-}$ mice

Effector CD62L$^{-/lo}$ CD4 T cells from 2.5-mo-old BXD2 or BXD2-*Rgs16*$^{-/-}$ mice were FACS-sorted and transferred into age/sex-matched BXD2-*Il17ra*$^{-/-}$ mice by i.v. injection (3 × 10^6 cells in 200 μl PBS per mouse). (**A**) Flow cytometry analysis of GL-7^{+}Fas^{+}GC B cells from the spleens of recipients on day 6. (**B**) ELISPOT assay of the autoantibody-producing B cells from the spleens of recipients on day 21. (**C**) The ratio of CD4^{+}-B220^{+} doublets versus CD4^{+}-B220^{-} singlets (left) and the ratio of CXCR5^{+}ICOS^{+} CD4^{+}-B220^{+} doublets versus CXCR5^{+}ICOS^{+} CD4^{+}-B220^{-} singlets (right) determined by flow cytometry sorting and analysis on day 6 in recipient spleens. Donor IL-17RA^{+} CD4 T cells and CXCR5^{+}ICOS^{+} T_{FH} cells were separated from IL-17RA^{-} recipient cells by IL-17RA staining. Ratios were calculated using the absolute cell count. (**D**) qRT-PCR analysis of *Rgs16* in conjugated and non-conjugated FACS-sorted CD4 T cells from BXD2 donor or BXD2-*Il17ra*$^{-/-}$ recipients on day 6. Data are representative (**A**) or indicate mean ± s.d. of two independent experiments with n = 3 mice per group; *p<0.05, **p<0.01, ***p< 0.005 between the groups (**B-D**).

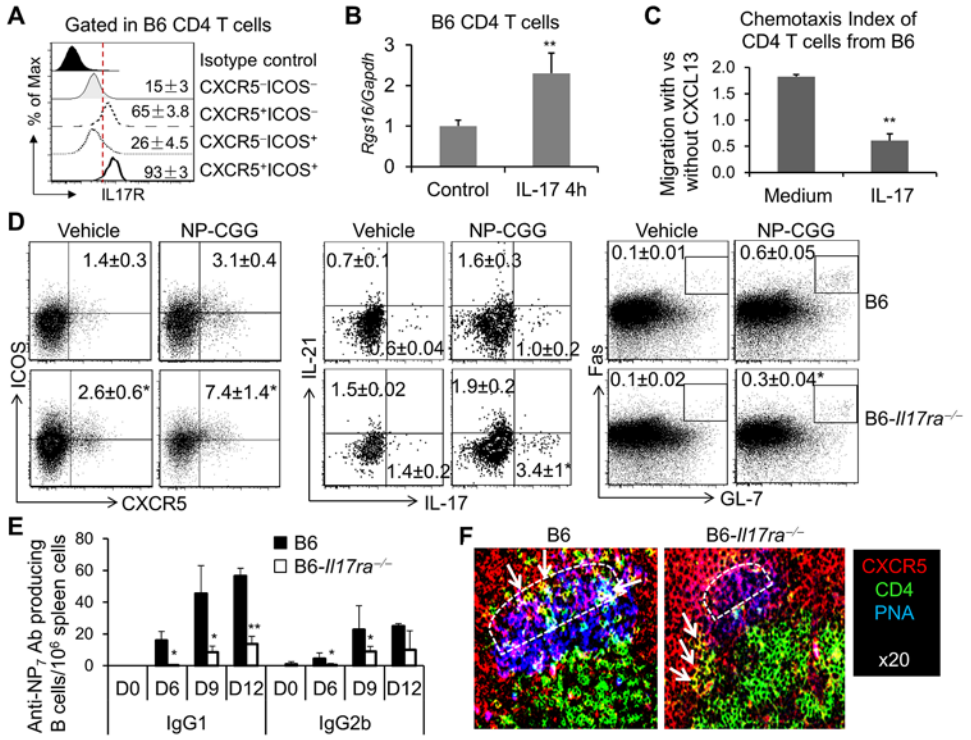

Figure 7. The increased percentage of T_{FH} cells in B6-*Il17ra*$^{-/-}$ mice also exhibited a lower ability to promote a TD immunization response

(**A**) FACS analysis of IL17RA in the indicated subsets. Cells were first gated for CD4 T cells. (**B**) qRT-PCR analysis of *Rgs16* in purified CD4 T cells with/without IL-17 (30 ng/ml) stimulation. (**C**) CXCL13 mediated chemotactic response of CD4 T cells with/without IL-17-pretreatment. (**D-F**) 2.5-mo-old B6 and B6-*Il17ra*$^{-/-}$ mice were immunized with NP (21)-CGG by i.p. Mice with vehicle injection were used as control. (**D**) Flow cytometry analysis of T_{FH} (left), expression of IL-21 and IL-17 in T_{FH} (gated on CXCR5^{+}ICOS^{+} CD4 T cells, middle) and GC B cells (gated on CD19^{+} cells, right) on day9 after NP-CGG immunization in the indicated mice. Numbers in quadrants indicate mean frequency ± s.d. (E) ELISPOT quantitation of the IgG anti-NP_7 antibody producing B cells at the indicated days (D) post NP-CGG immunization. (**F**) Confocal imaging on spleen tissue for GC B cells and T_{FH} on day 9. GC LZ is indicated by a white dashed line. Representative data (**A, D, F**) or indicate mean ± s.d. (**B, C, E**) are shown;*p < 0.05, ** p<0.01, ***p< 0.005. All experiments were carried out using 3 mice per group for two experiments (2.5 mo-old).